Hindawi
Journal of Food Biochemistry
Volume 2024, Article ID 5299378, 15 pages
https://doi.org/10.1155/2024/5299378

Research Article

Clam Peptides Attenuated Adenine-Induced Chronic Kidney Disease by Improving Inflammation, Oxidative Stress, and Intestinal Flora Composition

Wenping Ren,[1] **Qiaoni You**,[1] **Shanglong Wang**,[2] **Zimin Liu**,[2] **Shengcan Zou**,[2] **Xiang Gao**,[1] **and Yuxi Wei**[1]

[1]*College of Life Sciences, Qingdao University, Qingdao, China*
[2]*Chenland Nutritionals, Incorporated, Invine, California, USA*

Correspondence should be addressed to Xiang Gao; gaoxiang@qdu.edu.cn and Yuxi Wei; yuxiw729@163.com

Received 26 April 2023; Revised 8 February 2024; Accepted 16 February 2024; Published 4 March 2024

Academic Editor: Sanju Bala Dhull

Previously, we have prepared clam peptides (RBPs) that exhibited potential antihypertension and kidney protective effects in SHR rats by fermentation of *Ruditapes philippinarum* with *Bacillus natto*. In this study, we established an adenine-induced chronic kidney disease (CKD) in SD rats and investigated the improvement effects of RBPs on CKD. The results showed that compared with the model group, 8 weeks gavage of RBPs restored the structure of the kidney and reduced serum levels of CKD-related biochemical indicators, including NGAL, CR, Ca, UA, TG, IP, L-FABP, BUN, CHO, and cystatin C ($p < 0.05$). RBPs treatment also reduced serum levels of MDA, IL-1β, TGF-β1, and TNF-α and increased those of CAT and T-AOC ($p < 0.05$). In addition, the results of intestinal microbiota analysis showed that RBPs improved the intestinal flora composition by downregulating the proportion of *Firmicutes* and *Bacteroidetes*, decreasing the relative abundance of *Romboutsia*, *Ruminococcaceae_UCG-005*, and *Christensenellaceae_R-7_group* and increasing that of *Lactobacillus* and *Muribaculaceae* ($p < 0.05$). The results of this study indicated that RBPs can also be used as bioactive substances in marine drugs or functional foods to alleviate CKD.

1. Introduction

Kidney is an important organ responsible for metabolism in the human body, which is responsible for removing endogenous waste and maintaining acid-base and electrolyte balance in the body [1]. Numerous adverse factors, such as environmental pollution, family medical history, drug abuse, and metabolic diseases, will lead to chronic kidney disease (CKD) [2], which is defined as a sustained damage of renal parenchyma leading to chronic deterioration of renal function [3]. According to statistics, the incidence of CKD is continuously increasing around the world, and if not treated in time, it will develop into chronic renal failure, which will further weaken the detoxification ability of the kidney, leading to acid-base imbalance and endocrine disorders in the body [4].

At present, drug treatment is still the main therapeutic approach for CKD in clinic. However, drug treatment is always accompanied with side effects [5, 6]. For instance, long-term use of angiotensin-converting enzyme inhibitors may induce adverse reactions such as cough and angioedema [7]. The recurrence rate after cyclosporine treatment is more than 50%, and it can cause hypertension and nephrotoxicity [8]. Allopurinol and its derivatives may lead to skin allergy and other adverse reactions [9]. Thus, it is an inevitable trend to find safe and sideeffect-free natural food source products to help with the treatment of kidney disease. Among them, increasing evidence suggested that bioactive peptides play an effective role in the maintenance of renal function. For example, soy peptide attenuated renal dysfunction through anti-inflammation in adenine-induced CKD in mice [10]. *Perilla* peptides alleviated renal oxidative stress and chronic inflammation to improve adenine-induced CKD in mice, thereby improving renal injury [11].

Ruditapes philippinarum (*R. philippinarum*), commonly known as the clam, is widely distributed and ranks second among the bivalves in aquaculture worldwide [12]. It has been shown that peptides obtained after hydrolysis of *R. philippinarum* are biologically active in many aspects such as antioxidant activity, anticancer [13], antibacterial [14], and antihypertension [15]. In our previous study, we prepared peptides from *R. philippinarum* (RBPs) by *Bacillus natto* liquid fermentation. Briefly, 5% of total volume (v:v) *Bacillus natto* and 10% sucrose (compared to dried clam meat powder (w:w)) were added into the substrate of *R. philippinarum* (1 : 25 ratio of dried clam meat powder-to-water (w:w)) for fermentation at 45°C for 24 h. Subsequently, the fermentation products were centrifuged to separate the supernatant, which was freeze-dried to obtain RBPs [16]. We found RBPs significantly reduced blood pressures and restored renal injury in SHRs [16]. Inspired by these findings, we hypothesized that RBPs may improve adenine-induced CKD.

The adenine-induced CKD rodent model has much in common with the metabolic abnormalities of human CKD and has been frequently utilized to study the pathological basis of CKD [17, 18]. Therefore, in this study, we established an adenine-induced rat model of CKD to explore the improvement effect of RBPs on kidney damage and to provide a basis for high-value use of shellfish resources to produce marine drugs or functional foods that improve kidney function.

2. Materials and Methods

2.1. Experimental Animal. Male Sprague-Dawley (SD) rats (160–180 g) were purchased from Spafu (Beijing) Biotechnology Co., LTD. (SCXK (Beijing) 2019-0010). The feeding environment was 23–25°C, the relative humidity was 55–60%, and the light cycle was 12 h: 12 h. The experimental animals used in this study were all in accordance with international animal care guidelines and were approved by the Experimental Animal Center of Qingdao University.

2.2. Chemicals and Samples. Adenine (high purity, 98%) was supplied by Shanghai Yuanye Biotechnology Co., Ltd. Shenshuaining (SSN) capsules were obtained from Yunnan Lixiang Pharmaceutical Co., Ltd. RBPs were prepared from *R. philippinarum* by *Bacillus natto* fermentation at 45°C for 24 h, followed by membrane filtration and freezing-drying. Among them, peptides with a relative molecular mass of less than 2000 Da accounted for 90.47% [16]. Malondialdehyde (MDA), total antioxidant capacity (T-AOC), and catalase (CAT) kits were purchased from the Nanjing Jiancheng Bioengineering Institute. Neutrophil gelatinase-associated lipoprotein (NGAL), IL-1β, TGF-β1, TNF-α, Liver-fatty acid binding protein (L-FABP), and Cystatin C ELISA kits were obtained from Beijing Jingmei Biotechnology Co., Ltd.

2.3. Experimental Design. Fifty-four SD rats were kept in an environment of temperature (22 ± 3°C), humidity (65 ± 5%), and dark/light cycle for 12 h for one week. After the adaptation period, all rats were divided into two groups: normal group rats (Con, $n = 9$) gavaged with normal saline and model group rats (Mod, $n = 45$) gavaged with adenine (250 mg·kg^{-1}·d^{-1}). Both groups had free access to a normal diet. The systolic blood pressure (SBP) and the diastolic blood pressure (DBP) were measured by BP-2010A (Beijing Soft Invasive Biotechnology Co., Ltd.) at 2-week intervals [17]. After 3 weeks of the model building period, 6 model rats and 3 normal rats were randomly selected and sacrificed. Blood samples were collected from the abdominal aorta to detect the content of urea (UR), creatinine (CR), and uric acid (UA) in serum, and the model establishment was evaluated combined with the change in blood pressure. The rats with successful modeling were divided into five groups: model group (Con), orally gavaged with 10 mg·kg^{-1}·d^{-1} saline each day; SSN-treated positive control group (SSN), orally gavaged with 25 mg·kg^{-1}·d^{-1} SSN each day; and low-, medium-, and high-dose clam peptide-treated groups (RBPs-L, RBPs-M, and RBPs-H), orally gavaged with RBPs (50, 100, and 200 mg·kg^{-1}·d^{-1}). In the meanwhile, all groups were given a normal diet and intervened for 8 weeks. Their body weight was measured at the beginning of the trial and weekly thereafter.

2.4. Specimen Collection. After continuing treatment for 8 weeks, all rats were euthanized after 12 h fasting. Blood was collected from the abdominal aorta and centrifuged at 3500 r/min for 15 min to separate the serum. The heart, kidney, and liver were separated and weighed. The excised right kidney and part of the left kidney were wrapped in tinfoil and immersed in liquid nitrogen and frozen at −80°C until biochemical analysis. A small piece of the left kidney was placed in 4% formaldehyde fixative for histopathological examination. After the last blood pressure measurement, feces were collected from rats in a sterile environment. All serum, tissue, and feces were stored below −80°C until use.

2.5. Body Weight and Organ Index. During the treatment period of drug administration, the body weight of the rats was weighed weekly, and the body weight of the rats before sacrifice was recorded. After the rats were sacrificed, the kidneys, livers, and hearts of the rats were washed in 0.9% normal saline, wiped with filter paper, and weighed, and the organ index was calculated. The calculation formula is as follows: organ index = organ weight (g)/body weight (g).

2.6. Biochemical Tests in Plasma. The levels of NGAL, CR, Ca, UA, IP, blood urea nitrogen (BUN), and cholesterol (CHO) were measured by using an automatic biochemical analyzer. The levels of TGF-β1, IL-1β, NGAL, L-FABP, and Cystatin C in serum were detected by ELISA.

2.7. Histopathological Analysis of Renal Tissue. After immersion in 10% formalin for 2 days, dehydrated with alcohol, paraffin-fixed sections were stained with hematoxylin (HE) for histopathological analysis. Immunohistochemical sections were incubated with dialysate and blocking buffer,

with antibodies targeting genes, sequentially treated with peroxisome coupled streptavidin (Nichirei Co.) and 3, 3-diaminobenzidine tetrahydrochloride (DBA reagent), and finally stained with hematoxylin, and photographs were taken using a microscope. [16].

2.8. Gut Microbial Sequencing. All fecal samples were tested for gut microbial 16S rRNA by Shanghai Personal Biotechnology Co., Ltd., and high-throughput sequencing was performed on the Illumina NovaSeq platform.

2.9. Statistical Analysis. All results were expressed as the mean ± standard deviation, and one-way analysis of variance and Turkey's test were performed by using SPSS 18.0 statistical software. $p < 0.05$ and $p < 0.01$ were considered significant and had highly significant differences.

3. Results

3.1. Basic Information for the Model Being Successfully Built. At the end of three weeks, three rats from the Con and Mod groups were randomly selected and sacrificed for determination of UR, UA, and CR contents, and the results were shown in Figure 1. The results showed that adenine gavage treatment significantly increased the levels of UR, UA, and CR in serum (Figures 1(a)–1(c), $p < 0.05$), indicating that the CKD rat model was successfully established. Besides, their blood pressure was measured twice a week during the model building period, and the results were shown in Figures 1(d) and 1(e). The blood pressure of Mod rats was higher than that of normal rats, and there was a significant time-response relationship ($p < 0.05$). Therefore, this proved the success of modeling from another aspect.

3.2. RBPs Ameliorated Blood Pressures in CKD Rats. Blood pressure changes in rats during the 8-week RBPs intervention were shown in Figure 2. The SBP (a) and DBP (b) were dramatically higher in the Mod group than those in the Con group ($p < 0.05$). The blood pressure of rats in RBPs and SSN-treated groups showed a decline trend with the increase in administration days and gradually returned to the normal blood pressure range. At the end of treatment, SBP and DBP in the SSN and RBPs groups were lower than those in the Mod group ($p < 0.05$). Furthermore, a dose-dependent response was found in RBP-treated groups.

3.3. Effects of RBPs on Growth Parameters in CKD Rats. After successful modeling, the body weight of the Mod group was significantly lower than that of the Con group ($p < 0.05$), while there was no significant difference among the Mod group and the treatment groups ($p > 0.05$). After 8 weeks of treatment, changes in the body weight of the rats as well as organ indices were shown in Table 1. The body weight of the rats in the Mod group increased slowly, while that in the other treatment groups dramatically increased compared with the Mod group ($p < 0.05$). For organ indexes, the kidney, liver, and heart indexes of Mod rats increased by 53.73%, 14.29%, and 16.13%, respectively, compared with the Con group ($p < 0.05$). The kidney index, liver index, and heart index of the RBPs-H group were lower than those of the Mod group ($p < 0.05$). Although the organ indexes of SSN, RBPs-L, and RBPs-M groups showed a decreasing trend, there was no significant difference.

3.4. Effect of RBPs on the Renal Histopathology of CKD Rats. As shown in Figure 3(a), the kidneys of the normal group were in the shape of equine bean, with nail color obvious luster. In the model group, the exterior of the kidney was covered with white granules, and the whole kidney showed a frost-like appearance. After RBPs treatment, there was a trend of redness and a dose-dependent relationship. The therapeutic effect of the positive drug group was similar to that of the RBPs-M group, and the treatment effect of RBPs-H group was the most significant. The effect of RBPs on renal histopathology in rats was shown in Figure 3(b). Compared with the Con group, the renal tissue of the Mod group showed brown crystal deposition in the renal tubulointerstitial, a large number of dilated renal tubules, mesangial proliferation, glomerular atrophy, and inflammatory cell infiltration in the glomerulus. After administration, the above pathological changes were alleviated in the SSN group and high-, medium-, and low-dose RBPs groups. The brown crystals disappeared in the RBPs-M group and even completely in the RBPs-H group, and the renal tissue morphology was similar to that in the Con group. So the therapeutic effect of RBPs on renal tissue injury was dose-dependent.

3.5. RBPs Improved Serum Renal Function-Related Indices in CKD Rats. The results of serum biochemical indices of rats in each group were shown in Figure 4. Serum levels of NGAL, CR, Ca, IP, BUN, CHO, L-FABP, cystatin C, and UA were increased in the Mod group compared with the Con group ($p < 0.05$). After treatment with three different doses of RBPs, NGAL, CR, Ca, L-FABP, BUN, CHO, and cystatin C were significantly decreased compared with the Mod group ($p < 0.05$). Compared with the Mod group, the serum IP levels were decreased in RBPs-M and RBPs-H groups ($p < 0.05$) and UA levels also showed a downward trend in RBPs-H group ($p < 0.05$).

3.6. RBPs Attenuated Serum Oxidative Stress and Inflammation-Related Indices in CKD Rats. The oxidative stress-related indices of rats in each group were shown in Figures 5(a)–5(c). After adenine induction, the MDA level was significantly increased ($p < 0.05$) and CAT and T-AOC levels were significantly decreased ($p < 0.05$). Compared with the Mod group, RBPs-H and SSN groups had significant elevation of CAT and T-AOC and a reduction in MDA ($p < 0.05$). The RBPs-M group significantly reversed CAT and T-AOC ($p < 0.05$), but not MDA. There was no significant difference in the above indexes between the RBPs-L group and the Mod group.

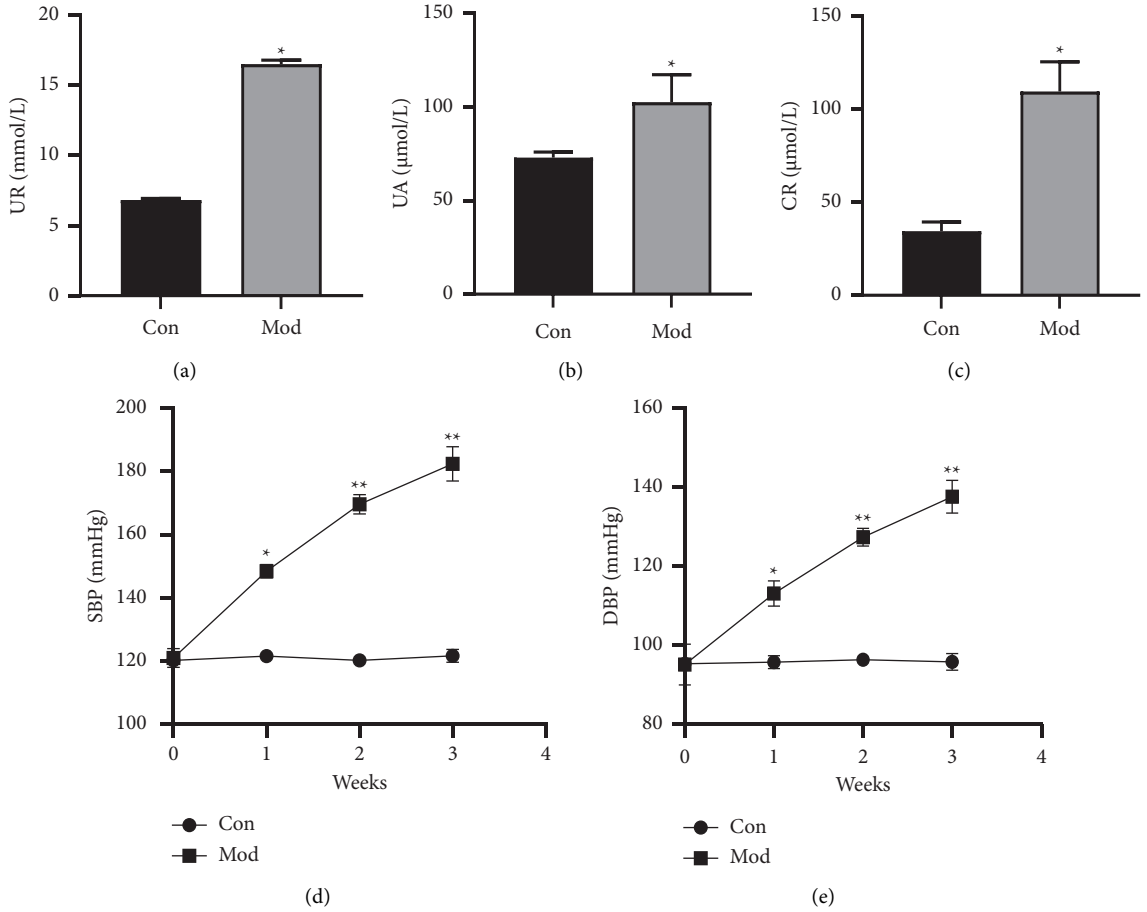

Figure 1: Changes of CKD-related indices in rats after adenine administration. (a) Serum levels of urea nitrogen (UR). (b) Serum levels of urea nitrogen (UA). (c) Serum levels of urea nitrogen (CR). (d) Changes in systolic blood pressure within three weeks of modeling. (e) Changes in diastolic blood pressure within three weeks of modeling (all data were presented as the mean ± SD; $^{*}p < 0.05$ vs. the Con group).

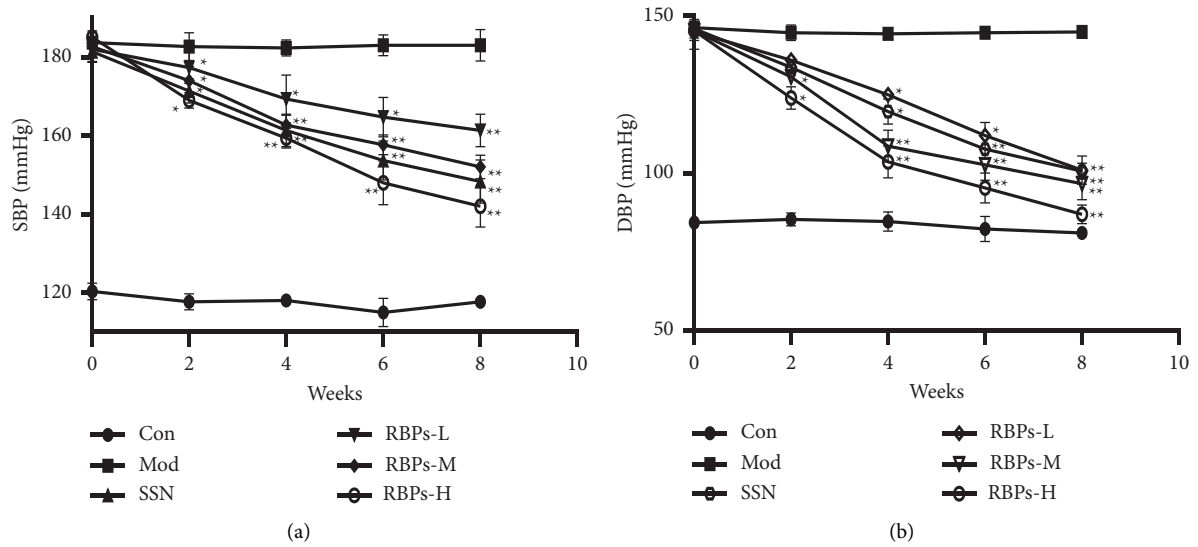

Figure 2: Effects of RBPs on blood pressure in rats during the eight-week treatment period. (a) Changes in systolic blood pressure in rats during the 8-week treatment period. (b) Changes in diastolic blood pressure in rats during the 8-week treatment period. All data were presented as the mean ± SD. Compared with the model group, $^{*}p < 0.05$; $^{**}p < 0.01$. Con: normal group; Mod: model group; SSN: Shenshuaining capsule-treated group; RBPs-L group: low-dose clam peptide-treated groups; RBPs-M group: medium-dose clam peptide-treated groups; RBPs-H group: high-dose clam peptide-treated groups.

Table 1: Effects of RBPs on body weight and organ indices in CKD rats.

Group	Body weight before treatment (g)	Body weight after treatment (g)	Kidney index ($\times 10^{-2}$)	Liver index ($\times 10^{-2}$)	Cardiac index ($\times 10^{-2}$)
Con	429.58 ± 28.11	513.47 ± 39.40	0.67 ± 0.09	2.31 ± 0.23	0.31 ± 0.04
Mod	368.28 ± 67.09*	422.24 ± 51.60*	1.03 ± 0.49*	2.64 ± 0.12*	0.36 ± 0.06*
SSN	390.37 ± 53.86	516.42 ± 78.30#	0.90 ± 0.21	2.64 ± 0.14*	0.32 ± 0.04
RBPs-L	390.27 ± 38.99	549.38 ± 53.70#	0.86 ± 0.16	2.51 ± 0.09	0.32 ± 0.02
RBPs-M	404.00 ± 24.67	541.57 ± 26.80#	0.76 ± 0.03	2.53 ± 0.12	0.32 ± 0.04
RBPs-H	422.82 ± 32.63	555.73 ± 53.30#	0.71 ± 0.09#	2.20 ± 0.25#	0.28 ± 0.01#

Note. All data were presented as the mean ± SD. $^{*}p < 0.05$, vs the Con group; $^{\#}p < 0.05$, vs the Mod group.

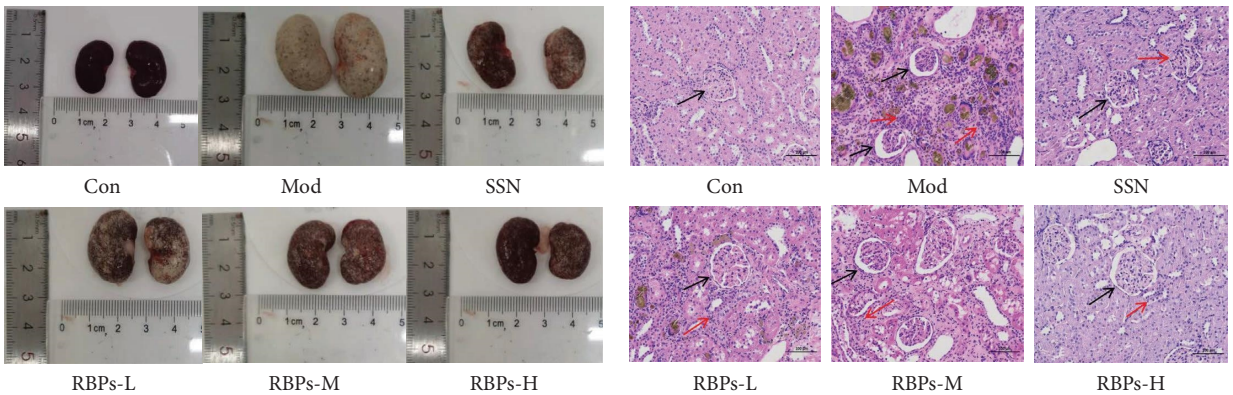

Figure 3: Effect of RBPs on the renal morphology and pathology of CKD rats. (a) Morphological change of rat kidneys from six experimental groups. (b) RBP treatment restored glomerular morphological changes (black arrows) and inflammatory infiltrates caused by renal injury (red arrows) in CKD rats. The scale bar was 100 μm.

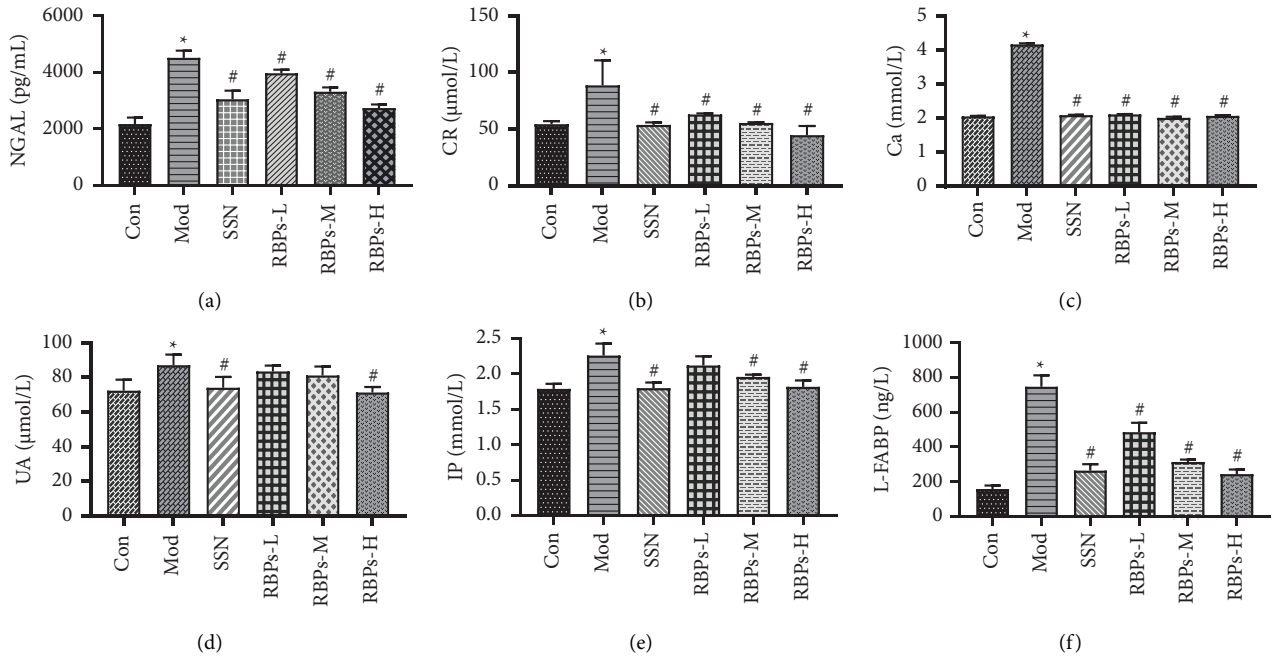

Figure 4: Continued.

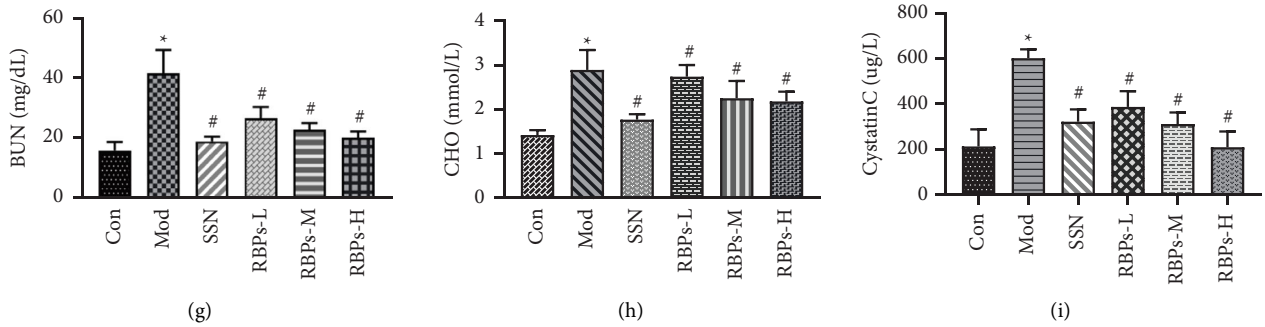

Figure 4: The effects of RBPs on NGAL (a), CR (b), Ca (c), UA (d), IP (e), L-FABP (f), BUN (g), CHO (h), and Cystatin C (i) levels in serum of adenine-induced CKD rats (all data were presented as the mean ± SD; $^{*}p < 0.05$ vs. the Con group; $^{\#}p < 0.05$ vs. the Mod group).

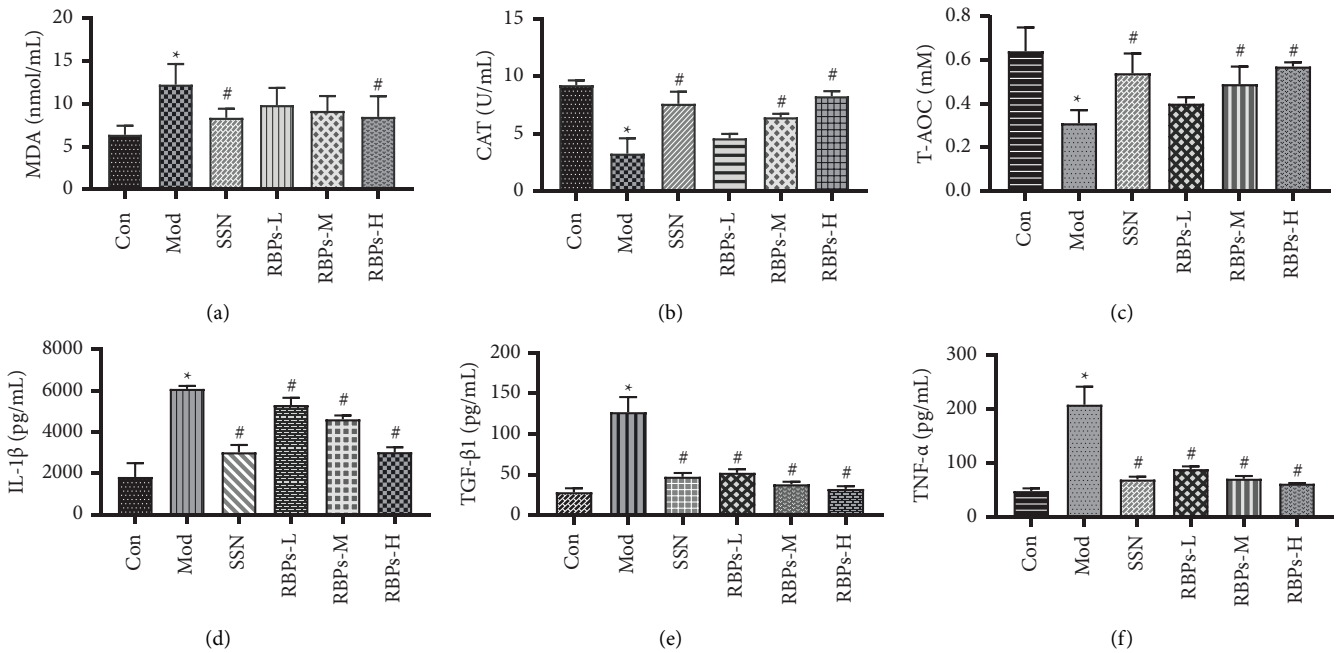

Figure 5: Effects of RBPs on oxidative stress and inflammation-related indices in serum. Serum levels of (a) MDA, (b) CAT, (c) T-AOC, (d) IL-1β, (e) TGF-β1, and (f) TNF-α (all data were presented as the mean ± SD; $^{*}p < 0.05$ vs. the Con group; $^{\#}p < 0.05$, vs the Mod group).

The results of serum inflammatory factors were shown in Figures 5(d)–5(f), Compared with the Con group, the levels of IL-1β, TGF-β1, and TNF-α in serum of the Mod group were significantly increased ($p < 0.05$). Both RBPs and SSN groups reduced the levels of IL-1β, TGF-β1, and TNF-α compared with the Mod group ($p < 0.05$). A dose-dependent relationship was noticed among the three RBPs groups.

3.7. Effects of RBPs on Gut Microbiota in CKD Rats

3.7.1. Sequence Splicing and Assembly. All stool samples in the six groups were sequenced with the use of Illumina sequencing platforms. A total of 2,218,135 qualified sequences were detected, which could be clustered into 24,430 OTUs for species classification under 97% similarity. Based on the annotation results of OTUs, 299 phyla, 52 classes, 1456 orders, 8040 families, 22097 genera, and 2189 species were obtained from the total samples of the 6 groups, as shown in Table 2.

3.7.2. Venn Analysis. To identify the number of common and unique OTUs between the experimental groups, Venn analysis was performed. As shown in Figure 6(a), there were 161, 186, 286, 328, and 375 OTUs overlapped with the Con group in Mod, SSN, RBPs-L, RBPs-M, and RBPs-H groups. A dose-dependent increasing trend was also observed in the RBPs groups. These results indicated that both RBPs and SSN increased the similarity of OTUs components to normal rats.

3.7.3. Alpha Diversity Analysis. Alpha diversity analysis indices were used to assess the species diversity of the microbial communities in experimental groups. The Chao1 index reflects the community richness, and the Shannon index shows the community diversity. As shown in Figures 6(b) and 6(c), compared with the Con group, the Chao1 index and Shannon index were lower in the Mod

Table 2: Sequencing information of intestinal bacteria in each group.

Group	Number of OTUs	Number of taxa of different taxonomic categories					
		Phylum	Class	Order	Family	Genus	Species
Con	5616	9	1	68	474	1748	149
Mod	3775	8	2	76	326	1175	80
SSN	3403	23	4	59	442	1462	139
RBPs-L	4002	19	3	46	355	1478	117
RBPs-M	4641	10	2	71	411	1721	156
RBPs-H	5548	21	2	75	611	1794	154
Total	24430	299	52	1456	8040	22097	2189

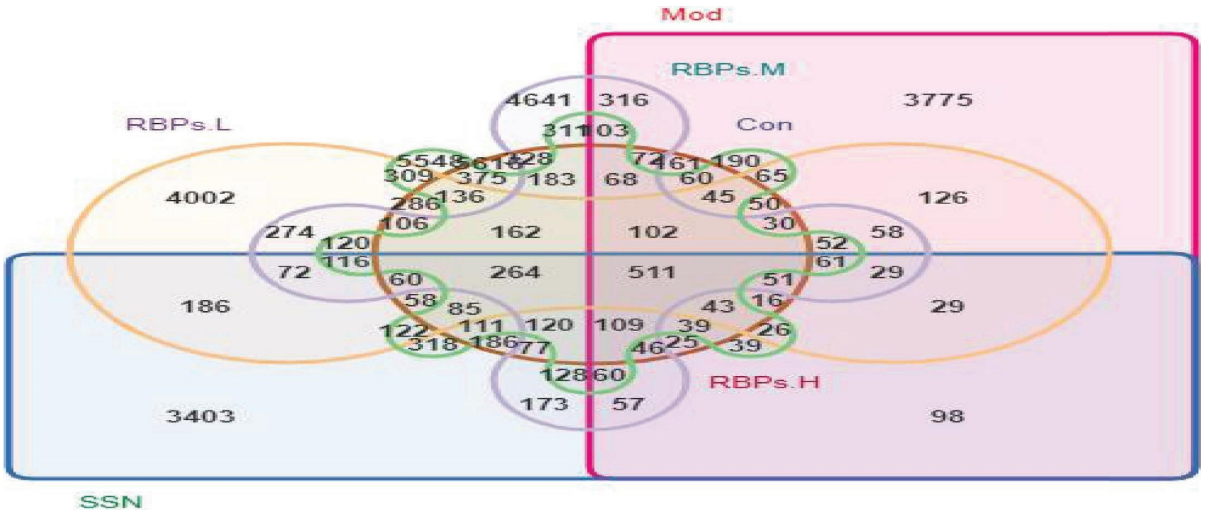

(a)

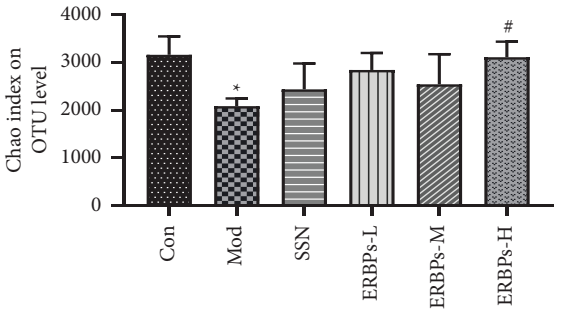

(b)

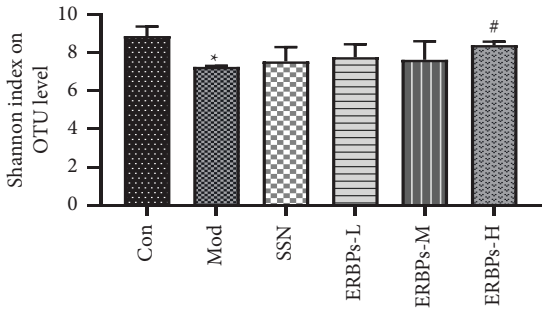

(c)

Figure 6: Continued.

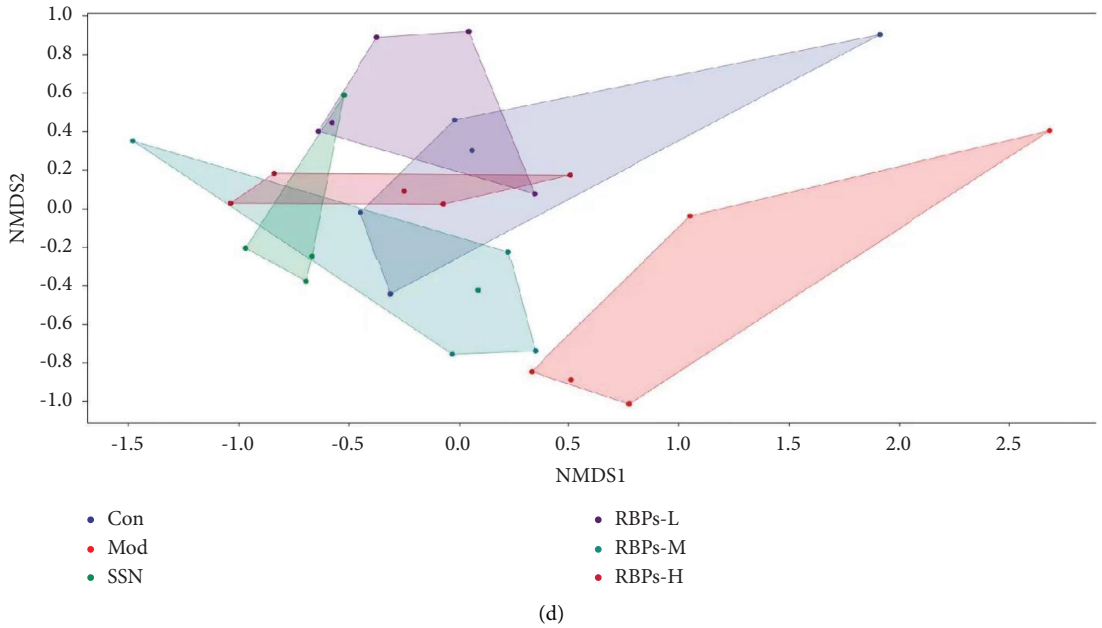

Figure 6: The effect of RBPs on fecal microbial composition in CKD rats. (a) Venn diagram. (b) Chao index. (c) Shannon index. (d) NMDS analysis (all data were presented as the mean ± SD; $^{*}p < 0.05$ vs. the Con group; $^{\#}p < 0.05$, vs the Mod group).

group, indicating decreased abundance and diversity of microbiota. With the increase of the RBPs dose, species diversity and colony richness in the RBPs group gradually increased, especially in the RBPs-H group, which was higher than that in the Mod group ($p < 0.05$). Therefore, RBPs can enhance the diversity of gut bacteria to a certain extent.

3.7.4. Beta Diversity Analysis—NMDS Analysis. Beta diversity analysis was used to determine differences in the structure of intestinal microbiota among experimental groups via NMDS analysis. The closer the face-space distance of each point, the smaller the difference in gut microbiota between groups. As shown in Figure 6(d), there was no overlap and a long distance between the Con and Mod groups, indicating that there was a significant difference in the composition of intestinal flora between the groups. This was followed by the SSN group, while the RBPs group was closer to the Con group, indicating that both SSN and RBPs significantly improved the gut microbiota composition in CKD rats.

3.7.5. Gut Microbiota Composition. The top 10 phyla were shown in Figures 7(a)–7(d). *Firmicutes* and *Bacteroidetes* were the two most important phyla. The decreased proportion of *Bacteroidetes* and the increased relative abundance of *Firmicutes* were found in the Mod group compared with the Con group. Compared with CKD rats, the proportion of *Bacteroidetes* at the phylum level was significantly increased after RBPs-M and RBPs-H treatments ($p < 0.05$), while *Firmicutes* significantly decreased ($p < 0.05$). No significant change was observed among RBPs-L and SSN on these two phyla. Furthermore, the ratio of *Firmicutes* and *Bacteroidetes* (F/B) was calculated. Both medium- and high-dose RBPs treatments reduced the elevated ratio of F/B in the Mon group ($p < 0.05$). There were no significant differences in other phyla among the groups.

Figure 7(e) showed the most abundant intestinal flora at genus levels in each group. Compared with the Con group, *Muribaculaceae* and *Lactobacillus* decreased and *Romboutsia*, *Ruminococcaceae_UCG-005*, and *Christensenellaceae_R-7_group* increased in the Mod group ($p < 0.05$). Intervention of RBPs decreased the relative abundance of *Romboutsia* and *Ruminococcaceae_UCG-005* compared to the Mod group ($p < 0.05$). Compared with the Mod group, the RBPs-M group displayed higher levels of *Lactobacillus* ($p < 0.05$). The relative abundance of *Muribaculaceae* was higher, and that of *Christensenellaceae_R-7_group* was lower in the RBPs-H group than in the Mod group. Compared with the Mod group, the SSN group displayed lower levels of *Romboutsia*, *Ruminococcaceae_UCG-005*, and *Christensenellaceae_R-7_group* and higher levels of *Lactobacillus* ($p < 0.05$) (Figures 7(f)–7(j)).

3.7.6. Correlation Analysis. Finally, we performed Spearman correlation analysis to analyze the associations between the relative abundance of significantly changed bacteria at phylum and genus levels among groups with CKD-related indices, and the results were shown in Figure 8. At the phylum level, *Firmicutes* were positively correlated with BUN, CHO, NGAL, L-FABP, cystatin C, Ca, IL-1β, TGF-β, and TNF-α ($p < 0.05$) but negatively correlated with CAT and T-AOC ($p < 0.05$). *Bacteroidetes* were negatively associated with CHO, NGAL, L-FABP, cystatin C, Ca, TGF-β, and TNF-α ($p < 0.05$) and positively related to CAT ($p < 0.05$). F/B was positively correlated with BUN, CHO, NGAL, L-FABP, cystatin C, MAD, TGF-β, and TNF-α

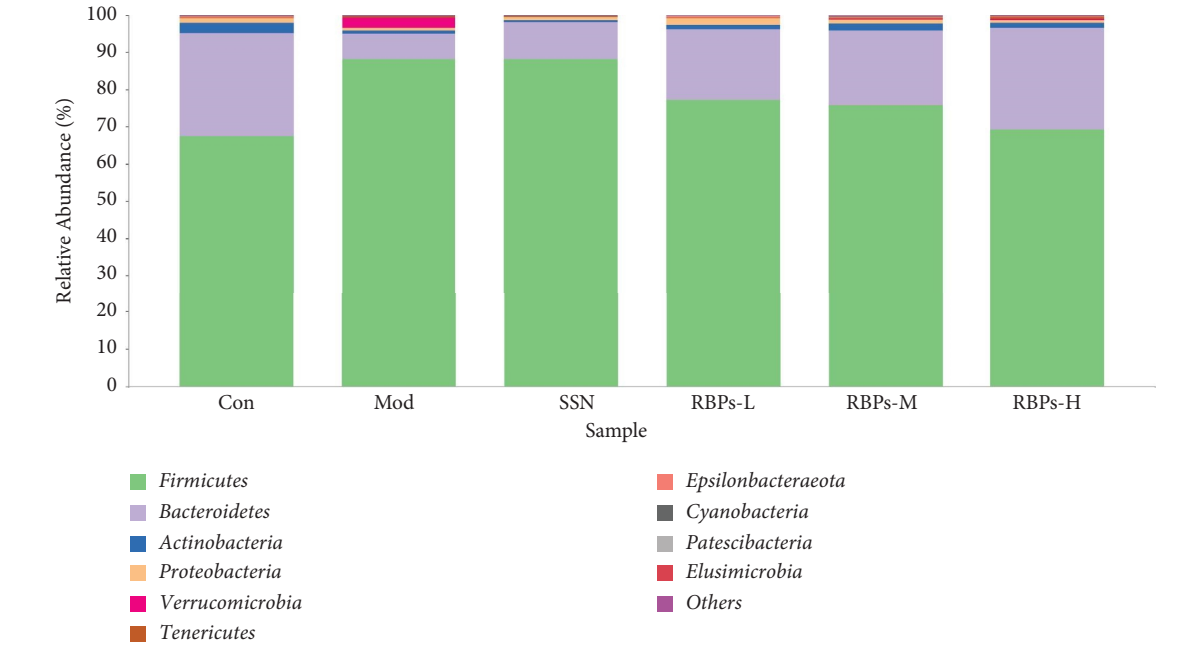

(a)

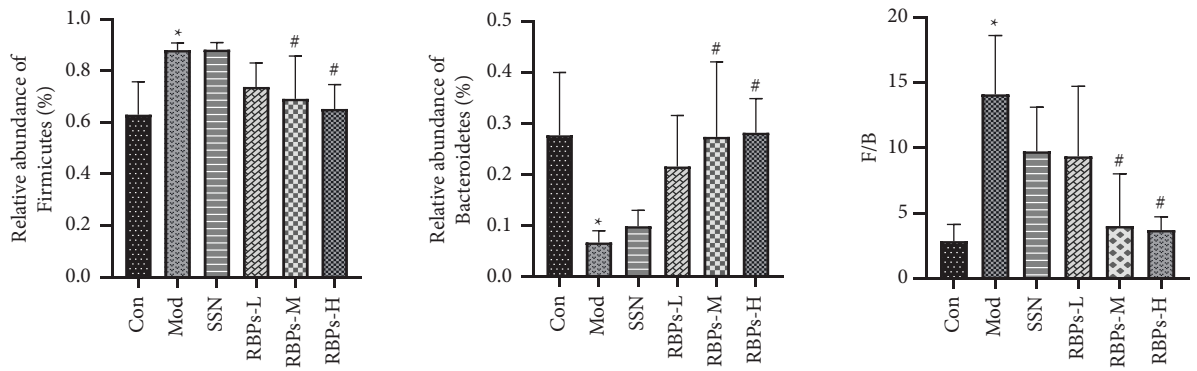

(b) (c) (d)

Figure 7: Continued.

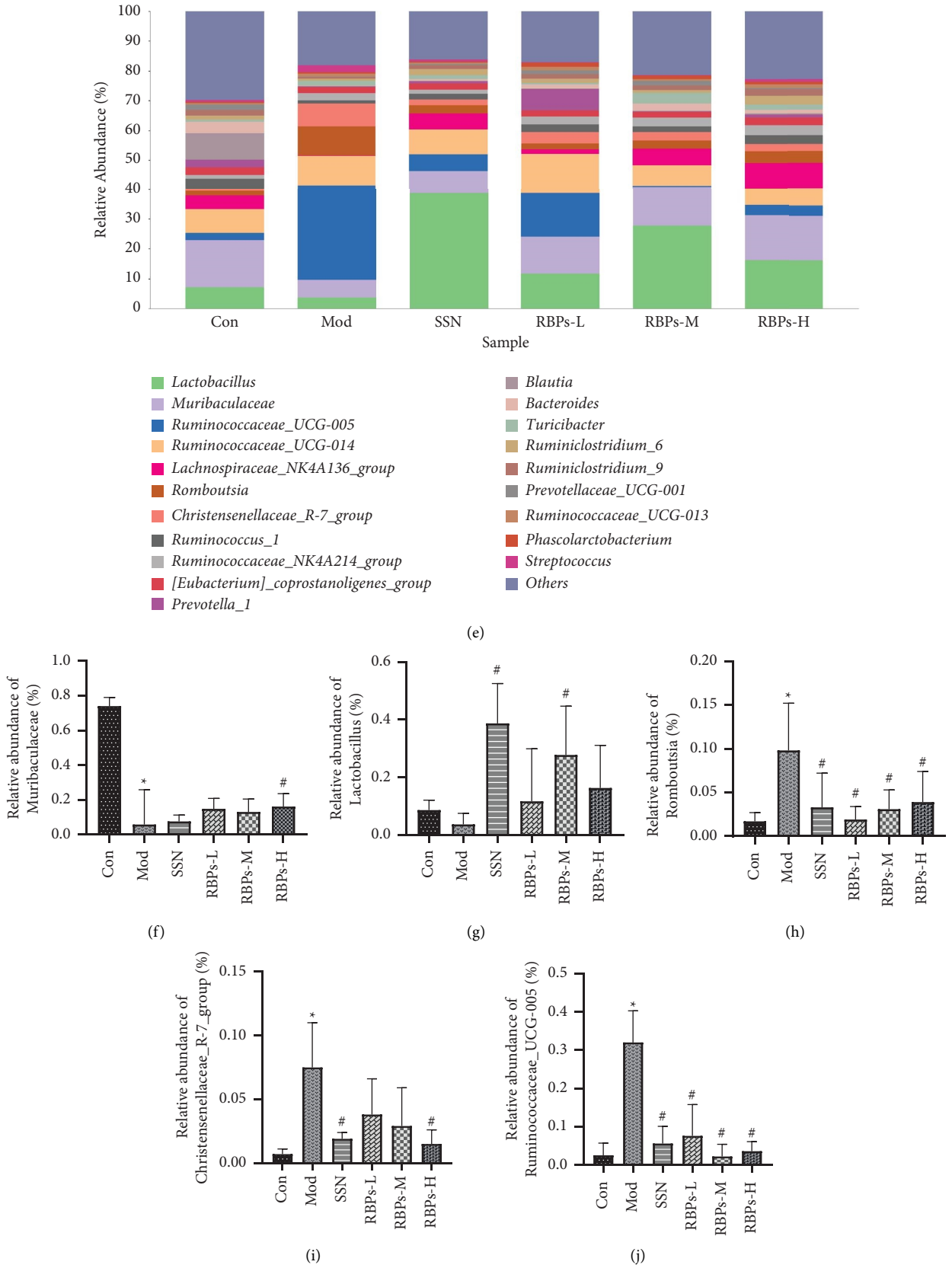

Figure 7: Gut microbiota composition at phylum and genus levels. (a) Composition of intestinal flora at phylum levels; (b) the relative proportion of *Firmicutes*; (c) the relative proportion of *Bacteroidetes*; (d) the ratio of *Firmicutes* and *Bacteroidetes* (F/B); (e) composition of intestinal flora at genus levels. (f–j) Relative abundance of *Muribaculaceae, Lactobacillus, Romboutsia, Christensenellaceae_R-7_group,* and *Ruminococcaceae_UCG-005* (all data were presented as the mean ± SD; $^{*}p < 0.05$ vs. the Con group; $^{\#}p < 0.05$ vs the Mod group).

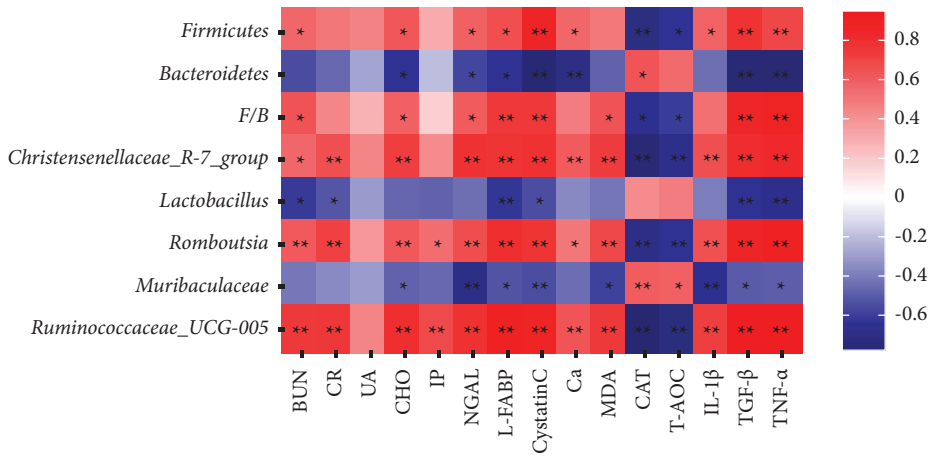

FIGURE 8: Correlations between gut microbiota at the phylum and genus levels with CKD-related parameters. Columns with symbols indicate significant differences in the correlation coefficient (r). $^{*}p < 0.05$; $^{**}p < 0.01$.

($p < 0.05$) and negatively associated with CAT and T-AOC ($p < 0.05$). At the genus level, *Christensenellaceae_R-7_group* was positively correlated with BUN, CR, CHO, NGAL, L-FABP, cystatin C, Ca, MAD, IL-1β, TGF-β, and TNF-α ($p < 0.05$) and negatively associated with CAT and T-AOC ($p < 0.05$). *Lactobacillus* was negatively correlated with BUN, CR, L-FABP, cystatin C, TGF-β, and TNF-α ($p < 0.05$). *Romboutsia* and *Ruminococcaceae_UCG-005* were positively correlated with BUN, CR, CHO, IP, NGAL, L-FABP, cystatin C, Ca, MAD, IL-1β, TGF-β, and TNF-α ($p < 0.05$) and negatively correlated with CAT and T-AOC ($p < 0.05$). *Muribaculaceae* was negatively associated with CHO, NGAL, L-FABP, cystatin C, MAD, IL-1β, TGF-β, and TNF-α ($p < 0.05$) and positively correlated with CAT and T-AOC ($p < 0.05$).

4. Discussion

A novel peptide named RBPs was prepared in our previous research by fermentation of *R. philippinarum* with *Bacillus natto* [19]. In this study, we proved for the first time that RBPs had significant therapeutic effects on adenine-induced CKD. Mechanism studies have shown that RBPs may repair renal injury by regulating the balance of oxidative status and inflammation and improving intestinal flora in CKD rats.

In previous studies, induction of CKD with adenine has been recognized as one of the most successful methods [15]. The effect of adenine-induced CKD is significant and conducive to observe. Long-term gavage of adenine can lead to chronic kidney injury similar to human, which is characterized by significant elevation in the serum levels of renal injury markers like CR, BUN, and UA [20]. In vivo, adenine is reduced to 2, 8-dihydroxyadenine, which enhances pressure on the capillaries around them by blocking the renal tubules, leaving them in a state of hypoxia, and then attaches to the renal tubules in the form of deposits, causing damage of renal tubular epithelial cells and leading to kidney diseases such as inflammation and fibrosis [21]. In this study, adenine was used to successfully induce the occurrence of CKD in rats. Subsequently, we found that RBPs protected against adenine-induced CKD in rats. In the body, UA can cause oxidative stress and inflammation, and the kidney is mainly responsible for the regulation of UA levels. Serum UR and CR are the most common indicators to assess CKD status [22]. In general, the kidney will exclude excess UA, CR, and UR in the body [11]. When the kidney is damaged, the blood levels of UA, CR, and UR will increase due to the inability to excrete them in time. NGAL is first found in the granules of human neutrophils, and its content is significantly increased in the blood during inflammation in many organs, like the kidney. L-FABP, as a lipid-binding protein, can bind fatty acids and transport them to mitochondria to provide energy for renal tubular cells. Both NGAL and L-FABP are markers used to predict the occurrence of early kidney injury [23, 24]. In addition, Cystatin C, as an endogenous cysteine peptidase inhibitor, has been intensively investigated as a biomarker of kidney function for many years [25]. When renal function is impaired, Cystatin C is freely filtered in the glomeruli and increased in blood. After RBP treatment, the elevated blood levels of UA, CR, UR, L-FABP, NGAL, and Cystatin C in the CKD rats were all significantly decreased, indicating the effectively protective effect of RBPs on kidney injury. Numerous previous reports indicated that peptides played CKD alleviative roles. For instance, *Perilla* peptides ameliorated kidney diseases by improving renal cell apoptosis and oxidative stress and maintaining intestinal barrier [11]. Soy peptide alleviates renal injury in hypertensive rats by activating the SIRT1-PGC1α/Nrf2 pathway [26]. Our study was the first to prove the CKD protective effect of peptides from *R. Philippinarum*.

The exact mechanisms of CKD are complex and largely unknown. However, it has been shown that CKD is closely related to oxidative stress and inflammatory response [27]. Oxidative stress and inflammation are linked with CKD by oxygen-derived free radicals, and the main pathological mechanism of which is characterized by the activity of intracellular and extracellular oxygen-derived free radicals causing kidney damage and then triggering an inflammatory response. First, free radicals usually interact with the molecular components of the nephron [28], causing a series of

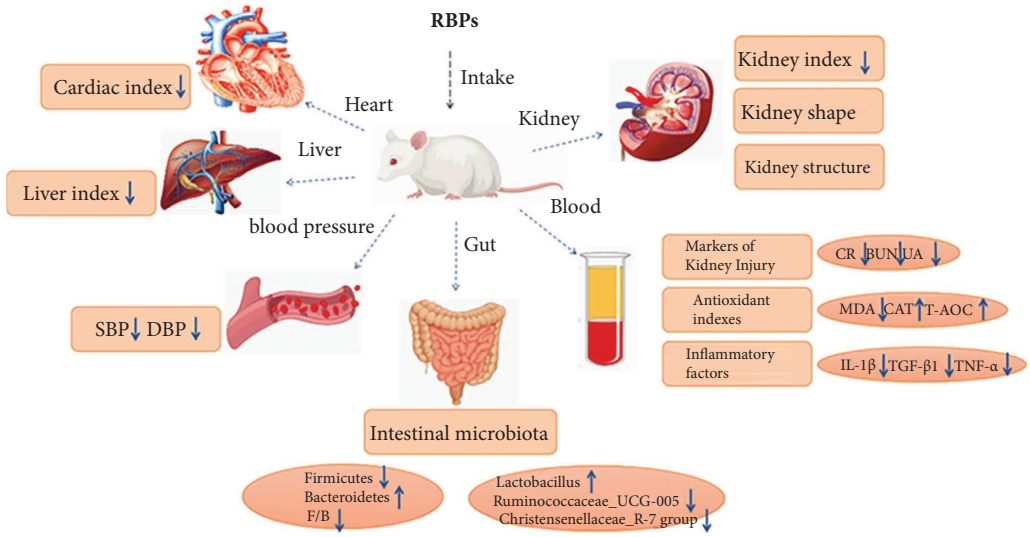

Figure 9: Potential mechanisms of the RBPs improving adenine-induced chronic kidney disease.

kidney damage reactions, such as lipid peroxidation of the cell membrane leading to membrane deactivation [29], kidney DNA breaking down and cross-links causing harmful mutations [30, 31], and oxidation of amino acids preventing some important functions [29]. Second, since free radicals interact with the nephron to produce secondary free radicals with the same harmful effects, the nephron will continue to be damaged [32], and the inflammatory response will stimulate the formation of additional free radicals. The damaged neutrophils were transferred across the membrane through the nicotinamide adenine dinucleotide phosphate oxidase system and coupled with molecular oxygen to produce superoxide [33]. Superoxide and free radicals and their targets continue to promote persistent renal inflammation [34]. Inflammatory signals promote the generation of reactive oxygen species (ROS) and cause nephron damage [31]. Finally, with long-term effects, the nephron interacting with free radicals starts to degrade gradually, and renal damage becomes more and more pronounced [35]. After adenine-induced CKD being built in this study, the activity of CAT, an antioxidant enzyme in renal tissue, thus caused peroxidative damage in renal tissue [36]. MDA is a product of peroxidation. The Serum T-AOC level is a commonly used indicator to reflect the overall antioxidant capacity in an organism [37]. After RBPs treatment, the serum level of MDA was increased and that of CAT and T-AOC in the CKD rats was enriched, indicating the antioxidant capacity was enhanced and renal oxidative damage was improved. TGF-β1 plays a regulatory role in renal fibrosis, and its level will increase during the development of CKD [38]. IL-1β and TNF-α as proinflammatory factors will also show an upward trend [39]. After RBPs treatment, the contents of IL-1β, TGF-β1 and TNF-α were decreased in the serum of CKD rats, indicating the notable anti-inflammatory effects of RBPs. Our results suggested that RBPs alleviated CKD by inhibition oxidative stress and inflammatory response.

The gut is rich in microbes that play critical roles in maintaining host health [40]. When renal function is impaired, it is often accompanied by changes in the composition of intestinal flora [41], and in turn, the changes in intestinal flora promote the development of CKD [42]. It has been shown that *Firmicutes* are positively correlated with plasma CR and BUN levels, while *Bacteroidetes* are negatively correlated with them [43]. The F/B ratio is usually used as a marker reflecting the condition of gut microbiota [44]. In our research, *Firmicutes* showed an upward trend in feces of CKD rats, while *Bacteroidetes* showed a downward trend, and the ratio of *Firmicutes* to *Bacteroidetes* (F/B) increased, which was consistent with previous reports [45]. After RBP treatment, the proportion of *Firmicutes* at the phylum level was reduced and the proportion of *Bacteroidetes* and F/B was increased, suggesting that RBPs could act by regulating the proportion of the microbiota. At the genus level, higher abundance of the genus *Muribaculaceae* was associated with lower levels of serum proinflammatory factors [46]. *Romboutsia*, *Christensenellaceae_R-7_group*, and *Ruminococcaceae_UCG-005* were reported to be enriched in the feces of CKD animals and were positively correlated with inflammation and oxidative stress [47–49]. In our study, RBPs treatment increased the fecal levels of *Muribaculaceae* and decreased *Romboutsia*, *Christensenellaceae_R-7_group*, and *Ruminococcaceae_UCG-005*, which are in line with the protective effect on CKD. *Lactobacillus* is beneficial bacteria that produce short-chain fatty acids (SCFAs). SCFAs can protect the kidney by preventing oxidative stress and inflammation in the kidney [50]. The proportion of *Lactobacillus* in the feces was increased after RBPs treatment, supporting the beneficial effect of RBPs on intestinal health. In addition, the correlation analysis also indicated that the modulated bacteria were significantly correlated with CKD-related indices. Beneficial bacteria (*Bacteroidetes*, *Muribaculaceae*, and *Lactobacillus*) were negatively correlated, while destructive bacteria (*Firmicutes*, *Romboutsia*, *Christensenellaceae_R-7_group*, and *Ruminococcaceae_UCG-005*) were positively correlated with kidney injury, oxidative stress, and inflammation. Overall, our finding suggested that the improvement effect of RBPs on adenine-induced CKD

might be at least partially attributed to the modulation of intestinal flora.

5. Conclusions

In conclusion, RBPs could improve CKD by protecting the structure of the kidney and reducing the serum levels of NGAL, CR, Ca, UA, TG, IP, L-FABP, BUN, CHO, and Cystatin C. Potential mechanisms might be lying in the enhancing of antioxidant capacity and anti-inflammation properties and restoring the composition of intestinal flora (as shown in Figure 9). Our results led novel insights for exploring RBPs as functional foods for CKD treatment.

Data Availability

The data that support the findings of this study are available on request from the corresponding authors.

Ethical Approval

All experimental animal use was approved by the Medical Ethics Committee of Affiliated Hospital of Qingdao University (QYFYWZLL25997, Qingdao, China).

Conflicts of Interest

The authors declare that there are no conflicts of interest regarding the publication of this paper.

Authors' Contributions

Wenping Ren was responsible for investigation, methodology, data analysis, validation, and writing the original draft. Qiaoni You was responsible for methodology and data analysis. Zimin Liu, Shanglong Wang, and Shengcan Zou were responsible for resources and validation. Xiang Gao was responsible for supervision, writing, reviewing, and editing. Yuxi Wei was responsible for conceptualization, supervision, funding acquisition, writing, reviewing, and editing. All the authors read and approved the final manuscript.

Acknowledgments

This research was funded by Taishan Industrial Leading Talents Project-Blue Talent Special.

References

[1] K. Cargill and S. Sims-Lucas, "Metabolic requirements of the nephron," *Pediatric Nephrology*, vol. 35, no. 1, pp. 1–8, 2020.

[2] J. Himmelfarb, "Linking oxidative stress and inflammation in kidney disease: which is the chicken and which is the egg?" *Seminars in Dialysis*, vol. 17, no. 6, pp. 449–454, 2004.

[3] G. Priyadarshini and M. Rajappa, "Predictive markers in chronic kidney disease," *Clinica Chimica Acta*, vol. 535, pp. 180–186, 2022.

[4] M. Long, Q. M. Li, Q. Fang, L. H. Pan, X. Q. Zha, and J. P. Luo, "Renoprotective effect of laminaria japonica polysaccharide in adenine-induced chronic renal failure," *Molecules*, vol. 24, no. 8, p. 1491, 2019.

[5] R. Y. Alhassani, R. M. Bagadood, R. N. Balubaid, H. I. Barno, M. O. Alahmadi, and N. A. Ayoub, "Drug therapies affecting renal function: an overview," *Cureus*, vol. 13, no. 11, Article ID e19924, 2021.

[6] J. Rani, S. B. Dhull, P. K. Rose, and M. K. Kidwai, "Drug-induced liver injury and anti-hepatotoxic effect of herbal compounds: a metabolic mechanism perspective," *Phytomedicine*, vol. 122, Article ID 155142, 2024.

[7] J. E. Lee and S. M. Bryant, "Unilateral angioedema," *The American Journal of Emergency Medicine*, vol. 49, pp. 302-303, 2021.

[8] M. W. Helmy, M. M. Helmy, and M. M. El-Mas, "Enhanced lipoxygenase/LTD4 signaling accounts for the exaggerated hypertensive and nephrotoxic effects of cyclosporine plus indomethacin in rats," *Biomedicine and Pharmacotherapy*, vol. 102, pp. 309–316, 2018.

[9] S. S. Gupta, N. Sabharwal, R. Patti, and Y. Kupfer, "Allopurinol-induced stevens-johnson syndrome," *The American Journal of the Medical Sciences*, vol. 357, no. 4, pp. 348–351, 2019.

[10] C. L. Tao, X. Xiang, W. K. Amakye, and J. Y. Ren, "Soy peptides ameliorate the progression of chronic kidney disease in mice via inhibition of inflammation," *Food Bioscience*, vol. 56, p. 10, 2023.

[11] M. L. Li, Y. Wei, M. Y. Cai, R. Z. Gu, X. C. Pan, and J. M. Du, "Perilla peptides delay the progression of kidney disease by improving kidney apoptotic injury and oxidative stress and maintaining intestinal barrier function," *Food Bioscience*, vol. 43, Article ID 101333, 2021.

[12] Y. Yamasaki, S. Taga, M. Kishioka, and S. Kawano, "A metabolic profile in Ruditapes philippinarum associated with growth-promoting effects of alginate hydrolysates," *Scientific Reports*, vol. 6, Article ID 29923, 2016.

[13] E. K. Kim, Y. S. Kim, J. W. Hwang et al., "Purification and characterization of a novel anticancer peptide derived from Ruditapes philippinarum," *Process Biochemistry*, vol. 48, no. 7, pp. 1086–1090, 2013.

[14] D. L. Yang, Q. Q. Zhang, Q. Wang et al., "A defensin-like antimicrobial peptide from the manila clam Ruditapes philippinarum: investigation of the antibacterial activities and mode of action," *Fish and Shellfish Immunology*, vol. 80, pp. 274–280, 2018.

[15] Y. Y. Chen, X. Gao, Y. X. Wei et al., "Isolation, purification and the anti-hypertensive effect of a novel angiotensin I-converting enzyme (ACE) inhibitory peptide from Ruditapes philippinarum fermented with Bacillus natto," *Food and Function*, vol. 9, no. 10, pp. 5230–5237, 2018.

[16] Y. H. Song, J. Yu, J. L. Song et al., "The antihypertensive effect and mechanisms of bioactive peptides from Ruditapes philippinarum fermented with Bacillus natto in spontaneously hypertensive rats," *Journal of Functional Foods*, vol. 79, Article ID 104411, 2021.

[17] B. H. Ali, M. Al Za'abi, S. A. Adham, J. Yasin, A. Nemmar, and N. Schupp, "Therapeutic effect of chrysin on adenine-induced chronic kidney disease in rats," *Cellular Physiology and Biochemistry*, vol. 38, no. 1, pp. 248–257, 2016.

[18] B. H. Ali, L. Cahlikova, L. Opletal et al., "Effect of aqueous extract and anthocyanins of calyces of Hibiscus sabdariffa (Malvaceae) in rats with adenine-induced chronic kidney disease," *Journal of Pharmacy and Pharmacology*, vol. 69, no. 9, pp. 1219–1229, 2017.

[19] B. H. Ali, M. Al Za'abi, S. A. Adham et al., "The effect of sildenafil on rats with adenine-Induced chronic kidney disease," *Biomedicine and Pharmacotherapy*, vol. 108, pp. 391–402, 2018.

[20] A. Mehmood, L. Zhao, M. Ishaq et al., "Renoprotective effect of stevia residue extract on adenine-induced chronic kidney disease in mice," *Journal of Functional Foods*, vol. 72, Article ID 103983, 2020.

[21] M. Karami, S. M. Owji, and S. M. S. Moosavi, "Comparison of ischemic and ischemic/reperfused kidney injury via clamping renal artery, vein, or pedicle in anesthetized rats," *International Urology and Nephrology*, vol. 52, no. 12, pp. 2415–2428, 2020.

[22] D. Pandya, A. K. Nagrajappa, and K. S. Ravi, "Assessment and correlation of urea and creatinine levels in saliva and serum of patients with chronic kidney disease, diabetes and hypertension- A research study," *Journal of Clinical and Diagnostic Research: Journal of Clinical and Diagnostic Research*, vol. 10, no. 10, pp. ZC58–ZC62, 2016.

[23] L. Holzscheiter, C. Beck, S. Rutz et al., "NGAL, L-FABP, and KIM-1 in comparison to established markers of renal dysfunction," *Clinical Chemistry and Laboratory Medicine*, vol. 52, no. 4, pp. 537–546, 2014.

[24] E. V. Schrezenmeier, J. Barasch, K. Budde, T. Westhoff, and K. M. Schmidt-Ott, "Biomarkers in acute kidney injury-pathophysiological basis and clinical performance," *Acta Physiologica*, vol. 219, no. 3, pp. 556–574, 2017.

[25] W. Ahn, T. H. Kim, T. Lee, J. O. Ahn, J. H. Choi, and J. Y. Chung, "Alteration of serum Cystatin-C levels after hemodialysis in dogs with kidney disease," *Pakistan Veterinary Journal*, vol. 41, no. 2, pp. 299–302, 2021.

[26] B. C. K. Tsai, D. J. Y. Hsieh, W. T. Lin et al., "Functional potato bioactive peptide intensifies Nrf2-dependent antioxidant defense against renal damage in hypertensive rats," *Food Research International*, vol. 129, Article ID 108862, 2020.

[27] Y. Chen, F. Cao, J. P. Xiao et al., "Emerging role of air pollution in chronic kidney disease," *Environmental Science & Pollution Research*, vol. 28, no. 38, pp. 52610–52624, 2021.

[28] M. P. C. Kao, D. S. C. Ang, A. Pall, and A. D. Struthers, "Oxidative stress in renal dysfunction: mechanisms, clinical sequelae and therapeutic options," *Journal of Human Hypertension*, vol. 24, no. 1, pp. 1–8, 2010.

[29] S. V. Avery, "Molecular targets of oxidative stress," *Biochemical Journal*, vol. 434, no. 2, pp. 201–210, 2011.

[30] M. D. Evans, M. Dizdaroglu, and M. S. Cooke, "Oxidative DNA damage and disease: induction, repair and significance," *Mutation Research: Reviews in Mutation Research*, vol. 567, no. 1, pp. 1–61, 2004.

[31] M. S. Cooke, M. D. Evans, M. Dizdaroglu, and J. Lunec, "Oxidative DNA damage: mechanisms, mutation, and disease," *The Federation of American Societies for Experimental Biology Journal*, vol. 17, no. 10, pp. 1195–1214, 2003.

[32] V. Cachofeiro, M. Goicochea, S. G. de Vinuesa, P. Oubiña, V. Lahera, and J. Luño, "Oxidative stress and inflammation, a link between chronic kidney disease and cardiovascular disease," *Kidney International- Supplement*, vol. 111, pp. S4–S9, 2008.

[33] J. Martensson, A. Holdfeldt, M. Sundqvist et al., "Neutrophil priming that turns natural FFA2R agonists into potent activators of the superoxide generating NADPH-oxidase," *Journal of Leukocyte Biology*, vol. 104, no. 6, pp. 1117–1132, 2018.

[34] L. Zhang, Y. Zhang, Z. Z. Wang et al., "Constructing metal-organic framework nanodots as bio-inspired artificial superoxide dismutase for alleviating endotoxemia," *Materials Horizons*, vol. 6, no. 8, pp. 1682–1687, 2019.

[35] E. Dounousi, E. Papavasiliou, A. Makedou et al., "Oxidative stress is progressively enhanced with advancing stages of CKD," *American Journal of Kidney Diseases*, vol. 48, no. 5, pp. 752–760, 2006.

[36] S. Colon, H. Y. Luan, Y. Liu, C. Meyer, L. Gewin, and G. Bhave, "Peroxidasin and eosinophil peroxidase, but not myeloperoxidase, contribute to renal fibrosis in the murine unilateral ureteral obstruction model," *American Journal of Physiology- Renal Physiology*, vol. 316, no. 2, pp. F360–F371, 2019.

[37] L. P. Mao, Q. Z. Qian, Q. Z. Li et al., "Lead selenide nanoparticles-induced oxidative damage of kidney in rats," *Environmental Toxicology and Pharmacology*, vol. 45, pp. 63–67, 2016.

[38] H.-J. Ki, S. Y. Kim, S. H. Lee et al., "Transforming growth factor-β receptor 2 gene polymorphisms are associated with end-stage renal disease," *Kidney research and clinical practice*, vol. 34, no. 2, pp. 93–97, 2015.

[39] K. Y. Lee, H. Y. Jung, D. Y. Yoo et al., "Dendropanax morbifera Leveille extract ameliorates D-galactose-induced memory deficits by decreasing inflammatory responses in the hippocampus," *Laboratory animal research*, vol. 33, no. 4, pp. 283–290, 2017.

[40] S. H. Jiang, S. Xie, D. Lv et al., "Alteration of the gut microbiota in Chinese population with chronic kidney disease," *Scientific Reports*, vol. 7, no. 1, p. 2870, 2017.

[41] J. P. Yang, Q. Li, S. M. Henning et al., "Effects of prebiotic fiber xylooligosaccharide in adenine-induced nephropathy in mice," *Molecular Nutrition and Food Research*, vol. 62, no. 15, Article ID e1800014, 2018.

[42] T. T. Cai, X. L. Ye, R. R. Li et al., "Resveratrol modulates the gut microbiota and inflammation to protect against diabetic nephropathy in mice," *Frontiers in Pharmacology*, vol. 11, p. 1249, 2020.

[43] M. Al-Asmakh, M. U. Sohail, O. Al-Jamal et al., "The effects of gum Acacia on the composition of the gut microbiome and plasma levels of short-chain fatty acids in a rat model of chronic kidney disease," *Frontiers in Pharmacology*, vol. 11, Article ID 569402, 2020.

[44] C. Han, Y. H. Jiang, W. Li, and Y. Liu, "Astragalus membranaceus and Salvia miltiorrhiza ameliorates cyclosporin A-induced chronic nephrotoxicity through the gut-kidney axis," *Journal of Ethnopharmacology*, vol. 269, Article ID 113768, 2021.

[45] Y. F. Zhu, H. D. He, Y. Y. Tang et al., "Reno-protective effect of low protein diet supplemented with a-ketoacid through gut microbiota and fecal metabolism in 5/6 nephrectomized mice," *Frontiers in Nutrition*, vol. 9, Article ID 889131, 2022.

[46] H. Q. Wang, J. Huang, Y. A. Ding et al., "Nanoparticles isolated from porcine bone soup ameliorated dextran sulfate sodium-induced colitis and regulated gut microbiota in mice," *Frontiers in Nutrition*, vol. 9, Article ID 821404, 2022.

[47] H. G. Wang, M. N. Zhang, X. Wen et al., "Cepharanthine ameliorates dextran sulphate sodium-induced colitis through

modulating gut microbiota," *Microbial Biotechnology*, vol. 15, no. 8, pp. 2208–2222, 2022.

[48] A. X. Zhuge, S. J. Li, Y. Yuan, B. Li, and L. J. Li, "The synergy of dietary supplements Lactobacillus salivarius LI01 and Bifidobacterium longum TC01 in alleviating liver failure in rats treated with d-galactosamine," *Food and Function*, vol. 12, no. 20, pp. 10239–10252, 2021.

[49] C. J. Hu, Y. L. Yan, F. J. Ji, and H. L. Zhou, "Maternal obesity increases oxidative stress in placenta and it is associated with intestinal microbiota," *Frontiers in Cellular and Infection Microbiology*, vol. 11, Article ID 671347, 2021.

[50] S. Q. Wang, D. Lv, S. H. Jiang et al., "Quantitative reduction in short-chain fatty acids, especially butyrate, contributes to the progression of chronic kidney disease," *Clinical Science*, vol. 133, no. 17, pp. 1857–1870, 2019.